# Dithiazolylthienothiophene Bisimide: A Novel Electron-deficient Building Unit for N-Type Semiconducting Polymers

*Yoshikazu Teshima,[†§] Masahiko Saito,[†§] Tomohiro Fukuhara,[‡] Tsubasa Mikie,[†] Kimihiro Komeyama,[†] Hiroto Yoshida,[†] Hideo Ohkita[‡] and Itaru Osaka*[,†]*

[†]Department of Applied Chemistry, Graduate School of Engineering, Hiroshima University, 1-4-1 Kagamiyama, Higashi-Hiroshima, Hiroshima, 739-8527, Japan

[‡]Department of Polymer Chemistry, Graduate School of Engineering, Kyoto University, Katsura, Kyoto, 615-8510, Japan

KEYWORDS: imide, semiconducting polymers, n-type, acceptor, organic field-effect transistors, organic photovoltaics

**ABSTRACT**

N-type (electron-transporting) semiconducting polymers are essential materials for the development of truly plastic electronic devices. Here, we synthesized for the first time dithiazolylthienothiophene bisimide (TzBI), as a new family for imide-based electron-deficient π-conjugated systems, and semiconducting polymers by incorporating TzBI into the π-conjugated backbone as the building unit. The TzBI-based polymers are found to have deep frontier molecular orbital energy levels and wide optical bandgaps compared to the dithienylthienothiophene bisimide (TBI) counterpart. It is also found that TzBI can promote the π–π intermolecular interactions of the polymer backbones relative to TBI most probably because the thiazole ring, which replaced the thiophene ring, at the end of the framework gives a more coplanar backbone. In fact, TzBI-based polymers function as the n-type semiconducting material in both organic field-effect transistor (OFET) and organic photovoltaic (OPV) devices. Notably, one of the TzBI-based polymers provides a power conversion efficiency of 3.3% in the all-polymer OPV device, which could be high for a low-molecular weight polymer (<10 kDa). Interestingly, while many of the n-type semiconducting polymers utilized in OPVs have narrow bandgaps, the TzBI-based polymers have wide bandgaps. This is highly beneficial for complementing the visible to near-IR light absorption range when blended with p-type narrow bandgap polymers that have been widely developed in the last decade. The results demonstrate great promise and possibility of TzBI as the building unit for n-type semiconducting polymers.

## INTRODUCTION

Semiconducting polymers are an important class of materials that can be used for organic electronic devices, such as organic light-emitting diodes (OLEDs), organic field-effect transistors (OFETs) and organic photovoltaics (OPVs), due to the solution-processability as well as the fascinating electronic properties.[1–6] The use of semiconducting polymers enables us to produce those devices by low-cost printing processes on light-weight and flexible plastic substrates. A large number of semiconducting polymers have been designed and synthesized in the last decade, which resulted in significant advances in the area.[7–9] While most of the chemists have devoted to developing hole-transporting (p-type) semiconducting polymers, electron-transporting (n-type) semiconducting polymers have been less investigated though they are equally essential to produce truly plastic devices such as logic circuits based on OFETs and all-polymer OPVs.[10–12] One main reason would be the lack of π-conjugated building units with strong electron-deficiency that ensures sufficiently deep lowest unoccupied molecular orbital (LUMO) energy levels for electron transport, although there are many electron deficient building units that function well for p-type semiconducting polymers.[13–15] In particular, with respect to the n-type semiconducting polymers (polymer acceptors) for OPV, the building units incorporated into those polymers are limited to several imide-functionalized units such as naphthalenediimide (NDI),[16] perylenediimide (PDI),[17] naphthodithiophenediimide (NDTI),[18] and dithienylthienothiophenebisimide (TBI),[19] isoindigo (iI),[20] and B←N bridged bipyridine (BNBP).[21] Thus, search for new electron-deficient building units that provide n-type semiconducting polymers is quite an important issue.

Imide-functionalized electron-deficient units have been studied quite intriguingly because of its strong electron-withdrawing nature,[22–24] which results in deep LUMO energy levels, thereby

enabling stable electron transport. Bithiophene imide (BTI) (Figure 1), where the imide group bridges bithiophene, is one of the attractive imide-functionalized units.[25] For example, a homopolymer of BTI has been reported to show relatively high electron mobilities of up to 0.038 $cm^2\ V^{-1}\ s^{-1}$ in OFETs.[26] Recently, related imide-bridged units such as thiazolylthiophene imide (TTzI),[27] bithiazole imide (BTzI),[28] and fluorinated BTI (F-BTI)[29] (Figure 1), which have higher electron-deficiency than BTI, have been synthesized. We have also reported on the synthesis of TBI (Figure 1), a doubly BTI-fused system, and TBI-based polymers, in which the polymers showed good n-type semiconducting properties with electron mobilities of ~0.05 $cm^2\ V^{-1}\ s^{-1}$ in OFETs as well as power conversion efficiencies (PCEs) of ~1% in all-polymer OPVs when combined with poly(3-hexylthiophene).[19] More recently, Guo and co-workers have synthesized difluorinated TBI (F-TBI) (Figure 1) and its copolymer, which showed high n-type semiconducting properties, particularly in all-polymer OPVs with PCEs of ~8%.[30] In addition, TBI-based polymers incorporating difluorinated thiophene as the comonomer afforded similarly high PCEs in all-polymer OPVs.[31]

Here, we report the synthesis of a novel electron-deficient unit dithiazolylthienothiophene bisimide (TzBI), in which thiophenes at the end of the TBI molecular structure were replaced by thiazoles (Figure 1), and TzBI-based polymers. Owing to the thiazole moieties, TzBI would have higher electron-deficiency and thus provide deeper LUMO and highest occupied molecular orbital (HOMO) energy levels relative to TBI. In addition, the absence of the hydrogen atom at the β-position of the outer ring would also beneficial to coplanarization of the polymer backbone and π–π intermolecular interactions. We will show the electronic properties and ordering structures in the thin film of the polymers. TzBI-based polymers indeed showed good n-channel property with electron mobilities of ~0.04 $cm^2\ V^{-1}\ s^{-1}$ in OFET devices. Furthermore, all-polymer OPV devices

that used TzBI-based polymers as the n-type material, combined with PTB7-Th as the p-type material, demonstrated power conversion efficiencies (PCEs) of ~3.3% despite the low molecular weights (<10 kDa), which indicates the great promise of TzBI as the building unit for n-type semiconducting polymers.

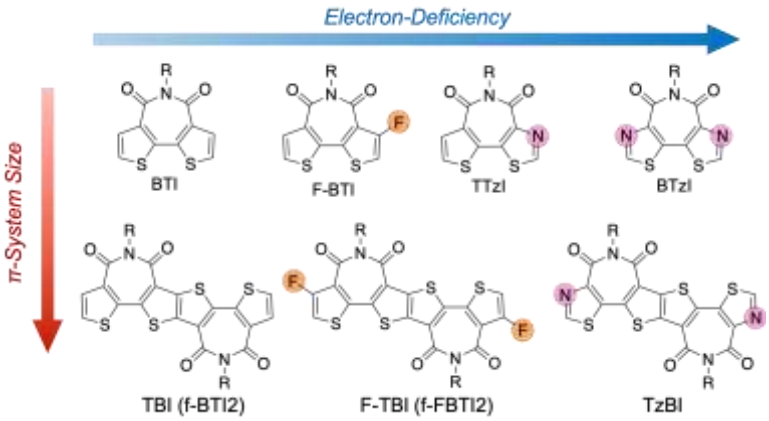


**Figure 1.** Chemical structure of the imide-bridged units.

## RESULTS AND DISCUSSION

### Monomer Synthesis and Polymerization.

Scheme 1 depicts the synthetic route to the TzBI-based polymers. 2-Amino-5-bromo-4-thiazole carboxylic acid ethyl ester (**1**) was deaminated via the Sandmeyer reaction to afford 5-bromo-4-thiazole carboxylic acid ethyl ester (**2**). **2** was then stannylated at the 5-position by treating with isopropylmagnesium chloride followed by tributhyltin chloride, which gave 5-tributylstannyl-4-thiazole carboxylic acid ethyl ester (**3**). The Stille coupling reaction of **3** with 2,5-dibromothieno[3,2-*b*]thiophene-3,6-dicarboxylic acid ethyl ether provided dithiazolylthienothiophene tetracarboxylic acid ethyl ester (**4**). **4** was then dibrominated at the 2-position of the thiazole moieties by the lithiation using lithium hexamethyldisilazide (LiHMDS) and the following treatment using 1,2-dibromo-1,1,2,2-tetrachloroethane, giving **5** almost quantitatively. It is noted that the 2-position of the thiazole moieties must be dibrominated using **4**. In fact, the bromination of TzBI by bromine or *N*-bromosuccinimide via the lithiation did not proceed (Scheme S1), though the bromination of TBI had proceeded well. This is most likely because the TzBI is too electron-deficient to allow electrophilic substitution and TzBI does not have sufficient solubility, even with long branched alkyl groups, at cryogenic temperature to allow lithiation reactions, respectively. Hydrolysis and subsequent cyclodehydration of **5** gave dithiazolylthienothiophene dicarboxylic anhydride (**6**). Finally, **6** was converted into dibrominated dithiazolylthienothiophene bisimide (TzBI-$Br_2$) via the amidation by 2-decyltetradecan-1-amine and the following cyclization in a good yield (92%).

Polymerizations of TzBI-$Br_2$ were carried out with distannylated thiophene and thienothiophene as comonomers via the Stille coupling reaction, which afforded PTzBIT and PTzBITT, respectively. The number average molecular weight ($M_n$) evaluated by high-

temperature gel-permeation chromatography (GPC) was 6.9 kDa with a polydispersity index (PDI) of 1.9 for PTzBIT and 7.6 kDa with a PDI of 2.2 for PTzBITT. The low molecular weight for the TzBI copolymers is possibly because of the low reactivity of TzBI-$Br_2$ under the normal conditions in the Stille coupling reaction. Both polymers had good solubility in common organic solvents such as chlorinated benzenes and toluene. Thermal properties of the polymers were studied by the differential scanning calorimetry (DSC) measurements. The DSC curves showed that the both polymers had no melting peaks below 350 °C (Figure S8).

**Scheme 1.** Synthetic route to TzBI-based polymers.

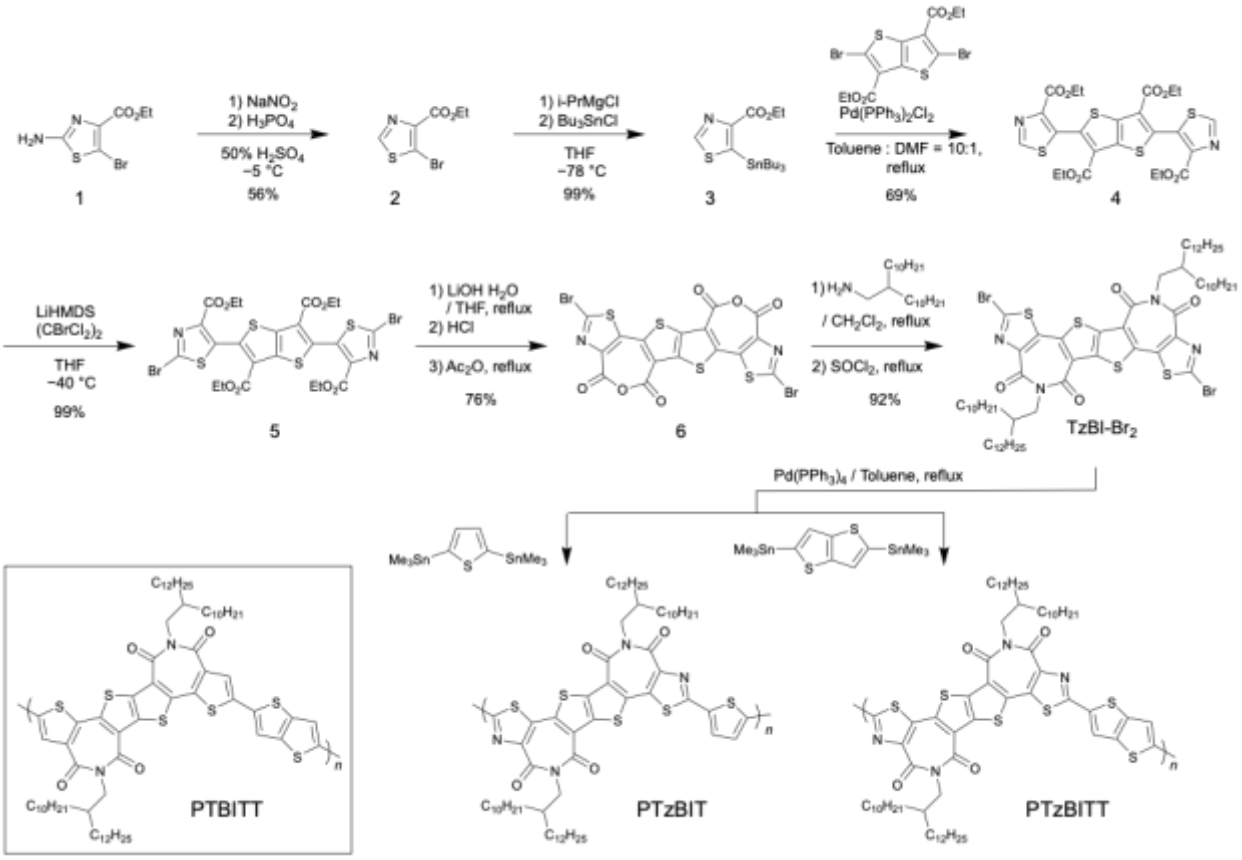

**Electrochemical and Optical Properties.**

Electronic structures of the polymers were studied by cyclic voltammetry and UV-vis absorption spectroscopy. Figure 2a shows the cyclic voltammograms of the polymers in thin film and Table 1 summarizes the HOMO and LUMO energy levels ($E_{HOMO}$ and $E_{LUMO}$) of the polymers determined from the onset oxidation and reduction potentials, respectively. While $E_{LUMO}$ of PTzBIT and PTzBITT was similar (−3.51 eV), $E_{HOMO}$ of PTzBIT (−6.26 eV) was deeper than that of PTzBITT (−6.14 eV). It is also noted that $E_{LUMO}$ and $E_{HOMO}$ of PTzBITT were deeper than those of PTBITT, a TBI-based polymer with the same thienothiophene co-unit, by 0.35 and 0.52 eV, respectively. This is most likely because only HOMO is located at the β-position of the thiophene rings in TBI and the nitrogen atoms of the thiazole rings in TzBI, and thus the electronic effect of the nitrogen atom is more pronounced on HOMO than LUMO in this system. It is also interesting to note that the HOMO–LUMO energy gap widened by replacing thiophene with thiazole, though it is possible to expect that the higher electron-deficiency of TzBI can make the donor–acceptor interaction along the polymer backbone larger and thereby can reduce the energy gap. This could be explained by the DFT calculations of the model compounds for TBI and TzBI (Figure 3). In both TBI and TzBI, HOMOs are mainly located on the dithienylthienothiophene and dithiazolylthienothiophene frameworks, whereas LUMOs are located on the imide groups as well as the frameworks. This can be viewed as that there is intramolecular donor–acceptor interactions in the TBI and TzBI moieties, where the frameworks act as the donor moiety and the imide groups act as the acceptor moiety. Therefore, TzBI has weaker intramolecular donor–acceptor interactions than TBI, which can widen the HOMO–LUMO energy gap. The fact that UV-vis spectrum of the TzBI unit showed a blue-shift compared to that of the TBI unit might support this hypothesis

(Figure S9). Overall, these results clearly indicate that TzBI possesses higher electron deficiency than TBI.

The UV-vis absorption spectra of PTzBIT and PTzBITT in both the solution and thin film are shown in Figures 2b and 2c, respectively, and the optical data are summarized in Table 1. In the solution, both polymers showed an absorption spectrum with two peaks, i.e., high-energy and low-energy bands. The absorption maximum ($\lambda_{max}$) in the low-energy band for PTzBIT and PTzBITT was observed at 579 and 597 nm, respectively, both of which were significantly blue-shifted from that for PTBITT (652 nm). The blue-shift in the absorption in PTzBITT, as well as PTzBIT, compared to PTBITT is in good agreement with the results in CV, in which the HOMO–LUMO energy gap widened and the $E_{HOMO}$ was deepened more significantly than the $E_{LUMO}$. The slight red-shift of the absorption range in PTzBITT relative to PTzBIT is attributable to the extended π-electron system in the thienothiophene co-unit compared to the thiophene co-unit. In the thin film, the absorption bands were mostly the same as those in the solution, in which for example the low-energy band for PTzBIT and PTzBITT was 587 and 602 nm, respectively. Thus, the optical bandgap ($E_g^{opt}$) calculated using the absorption onset ($\lambda_{edge}$) in the thin film was 1.96 eV for PTzBIT and 1.90 eV for PTzBITT. This implies that the backbone coplanarity is inherently high even in the isolated state. Interestingly, while most widely studied n-type semiconducting polymers based on NDI possess narrower optical bandgaps, the TzBI-based polymers had such wide optical bandgap. This is highly beneficial for complementing the visible range by combining with widely studied p-type semiconducting polymers with narrow optical bandgaps.

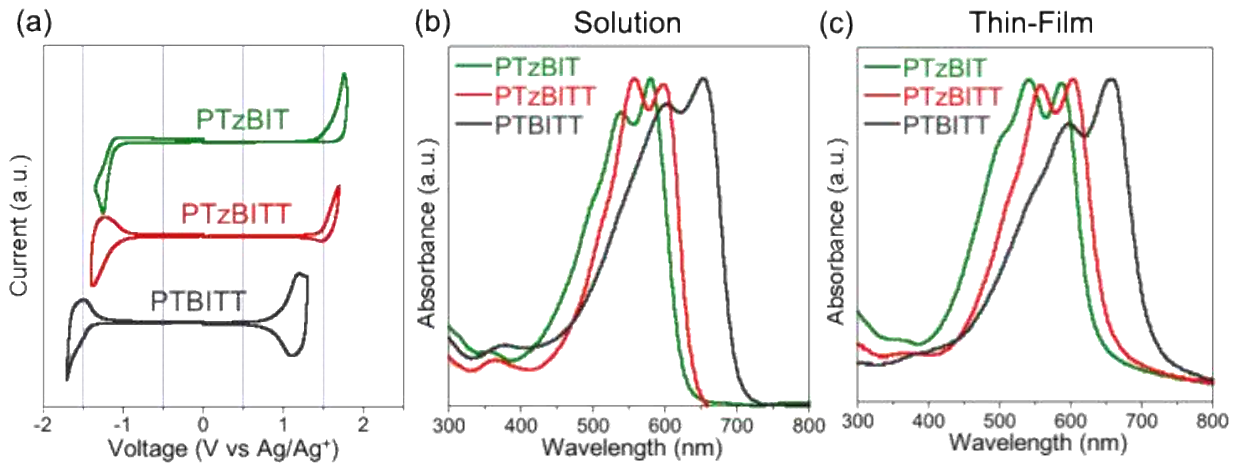


**Figure 2.** (a) Cyclic voltammograms of the polymers in thin film. (b, c) UV-vis absorption spectra of the polymers: (b) chlorobenzene solution, (c) thin film.

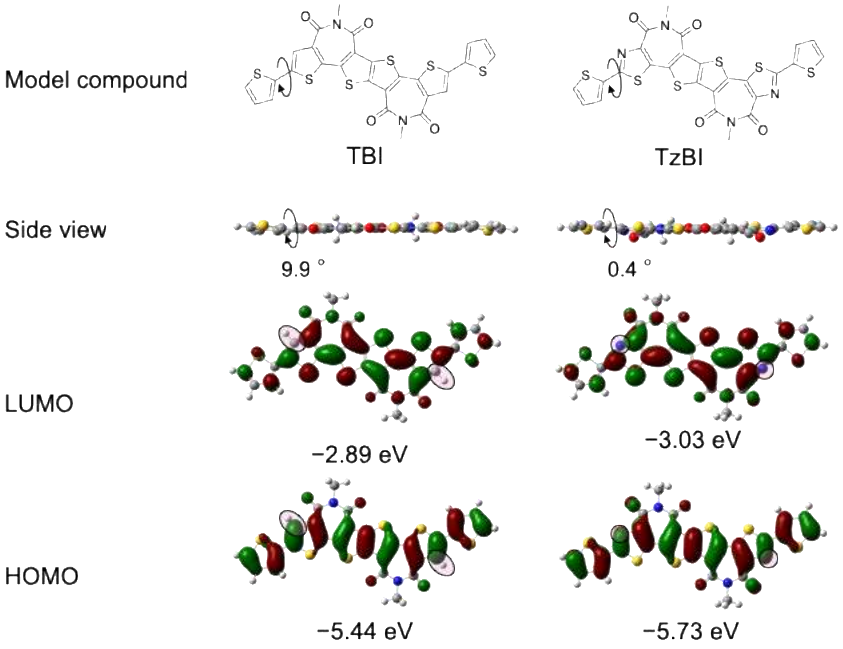


**Figure 3.** Side view for the optimized structure and geometry of LUMOs and HOMOs for the optimized structure of the model compounds based on TBI and TzBI (DFT method at the B3LYP/6-31g(d) level).

**Table 1.** Electrochemical and optical properties of the polymers

| Polymer | $E_{HOMO}$ (eV)[a] | $E_{LUMO}$ (eV)[b] | $\lambda_{max}$ (nm)[c] | | $\lambda_{edge}$ (nm)[d] | $E_g^{opt}$ (eV)[e] |
|---|---|---|---|---|---|---|
| | | | Sol. | Film | | |
| PTzBIT | −6.26 | −3.51 | 538, 579 | 539, 587 | 633 | 1.96 |
| PTzBITT | −6.14 | −3.55 | 558, 597 | 557, 602 | 652 | 1.90 |
| PTBITT | −5.65 | −3.27 | 600, 652 | 597, 658 | 714 | 1.74 |

[a]HOMO energy level. [b]LUMO energy level. [c]Absorption maximum in solution and thin film. [d]Absorption edge in thin film. [e]Optical bandgap estimated from the absorption edge.

**Polymer Ordering Structure in the Thin Film**

The grazing incidence X-ray diffraction (GIXD) measurement was carried out for PTzBIT and PTzBITT neat films to investigate the ordering structure. The two-dimensional (2D) GIXD patterns and the cross-sectional profiles along the $q_z$ axis (out-of-plane: OOP) and $q_{xy}$ axis (in-plane: IP) are shown in Figure 4. A diffraction corresponding to the π–π stacking structure appeared on the $q_z$ axis for PTzBIT ($q_z \approx 1.79$ Å$^{-1}$), in which the *d*-spacing ($d_\pi$) was calculated to be 3.55 Å. In PTzBITT, however, the π–π stacking diffraction was observed on the $q_{xy}$ axis, and $d_\pi$ was found to be 3.51 Å ($q_{xy} \approx 1.77$ Å$^{-1}$). These results indicate that whereas PTzBIT formed the face-on orientation, PTzBITT formed the edge-on orientation. This probably arises from the higher intermolecular interactions in PTzBITT, which is evident from the fact that PTzBITT had lower solubility than PTzBIT, and that $d_\pi$ for PTzBITT was somewhat shorter than that for PTzBIT.[32]

It is noted that although PTzBITT had a low molecular weight, the $d_\pi$ was similar to that of the TBI counterpart (PTBITT) that had much higher molecular weight (Figure S2). Further, the crystallinity was even higher for PTzBITT than for PTBITT, as the coherence length calculated using the modified Scherrer's equation ($2\pi$/fwhm)[33] from the diffraction corresponding to the π–π stacking structure for PTzBITT was 4.7 nm, which was larger than that for PTBITT (4.3 nm). This suggests that TzBI offers higher crystallinity relative to TBI. This is most likely due to the enhanced coplanarity of the backbone as shown by the computation that the dihedral angle between the TzBI moiety and the neighboring thiophene ring is calculated to be 0.4°, which is significantly smaller than 9.9° for the case in TBI. This would originate in the reduced steric hindrance by the absence of the hydrogen atom in the outer ring (thiazole) of TzBI.

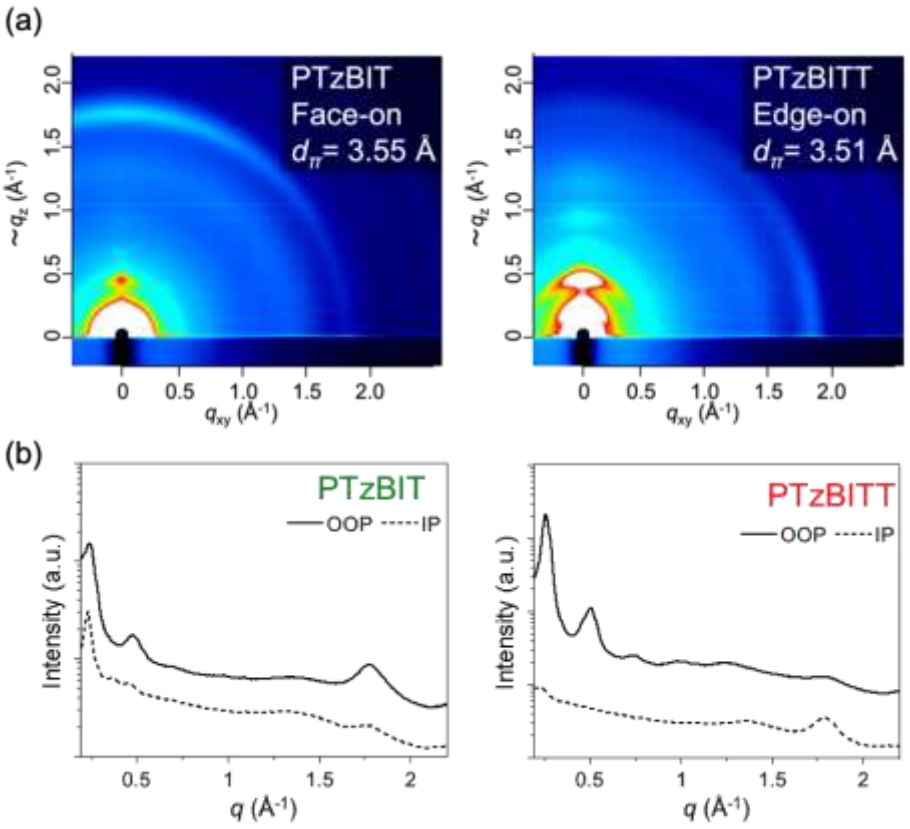


**Figure 4.** (a) 2D GIXD patterns of the polymer neat films. (b) Cross-sectional profiles cut along the $q_z$ axis (out-of-plane: OOP) and $q_{xy}$ axis (in-plane: IP) direction of the 2D GIXD patterns.

**Device Properties**

We fabricated OFET devices that used PTzBIT and PTzBITT, both of which showed typical n-channel behavior. Figures 5a and 5b display transfer and output curves of the devices after annealing the polymer films at 200 °C. While PTzBIT showed relatively low electron-mobility ($\mu_e$) of $1.1 \times 10^{-3}$ $cm^2$ $V^{-1}$ $s^{-1}$, PTzBITT showed reasonably high $\mu_e$ of 0.038 $cm^2$ $V^{-1}$ $s^{-1}$ (Table 2). The current on/off ratios ($I_{on}/I_{off}$) for the both polymer devices were fairly large ($10^6$–$10^7$) (Table 2). The higher $\mu_e$ observed for PTzBITT than for PTzBIT was consistent with the fact PTzBITT formed preferential edge-on orientation whereas PTzBIT formed face-on orientation. It is also noted that the $\mu_e$ of PTzBITT was similar to that of PTBITT even though the molecular weight was much lower. This is likely due to the enhanced crystallinity in PTzBITT compared to that in PTBITT. The result suggests that TzBI-based polymers have good potential as the n-type semiconducting material.

We also fabricated all-polymer OPV devices with an inverted structure (ITO/ZnO/PTB7-Th:TzBI-based polymer/$MoO_x$/Ag). Since the TzBI-based polymers had wide optical bandgaps, we chose PTB7-Th with a narrow bandgap of 1.58 eV as the p-type semiconducting polymer to capture as much incident light as possible. The photoactive layer was fabricated by spin-coating the chloroform solution of the polymer blend with a p:n weight ratio of 1:1. The energy diagrams of the materials, as depicted in Figure 6a, show that the energetics are well-aligned between PTB7-Th (p-type material) and TzBI-based polymers (n-type materials), in which the offset energies of LUMOs and HOMOs are sufficiently large to trigger the photo-induced charge transfer. Figures 6b and 6c display the current density ($J$)–voltage ($V$) curves and external quantum efficiency (EQE) spectra of the cells, respectively, and Table 2 summarizes the photovoltaic properties of the cells. The PTzBIT cell barely showed photovoltaic performance with a PCE of less than 1%.

Nevertheless, the photoresponse was observed in the visible region covering 400–800 nm, indicating that both PTzBIT and PTB7-Th functioned as photoactive materials. The PTzBITT cell showed reasonably high photovoltaic performance with a PCE of as high as 3.30% ($J_{SC}$ = 8.61 mA $cm^{-2}$, $V_{OC}$ = 0.96 V, FF = 0.40). Importantly, EQE at the PTzBITT absorption band was similarly high as that at the PTB7-Th absorption band, indicating that PTzBITT largely contributed to the photovoltaic performance of the cell.

Importantly, the photovoltaic performance of the TzBI polymers, even PTzBIT, was higher than that of PTBITT (Figure S12, Table S3). This should be ascribed to the deeper $E_{LUMO}$ of the TzBI polymers and thereby the relatively large offset of the $E_{LUMO}$s between PTB7-Th and the TzBI polymers than that between PTB7-Th and PTBITT, which again allows sufficient driving force for photo-induced electron transfer. To confirm this, we conducted the photoluminescence (PL) quenching study. Figure 7 shows the PL spectra of the PTB7-Th/PTzBITT and PTB7-Th/PTBITT blend films along with the PTB7-Th neat film excited at 730 nm. It is clear that the PL intensity was much lower in the PTB7-Th/PTzBITT blend film than in the PTB7-Th/PTBITT blend film, indicating that PL from PTB7-Th was quenched more efficiently in the PTB7-Th/PTzBITT blend film. This suggests that the electron transfer is more efficient in the PTB7-Th/PTzBITT blend than in the PTB7-Th/PTBITT blend.

It is noted that, in the blend film, only the diffractions corresponding to PTB7-Th were observed and those corresponding to the TzBI polymers as well as PTBITT were not observed (Figure S9), suggesting that both the TzBI polymers and PTBITT are similarly disordered in the blend film. This implies that the improved photovoltaic performance in PTzBITT compared to PTBITT is largely attributed to the enhanced electron-deficiency (lower LUMO energy level). In addition, the

disordered structure of PTzBITT and PTzBIT in the blend film could be because of their low molecular weights. Such disordered structure might be one of the reasons for the relatively low $J_{SC}$ and FF of the cells. Thus, further improvement of the molecular weight is highly required for improving the performance of the all-polymer OPVs based on the TzBI-based polymers.

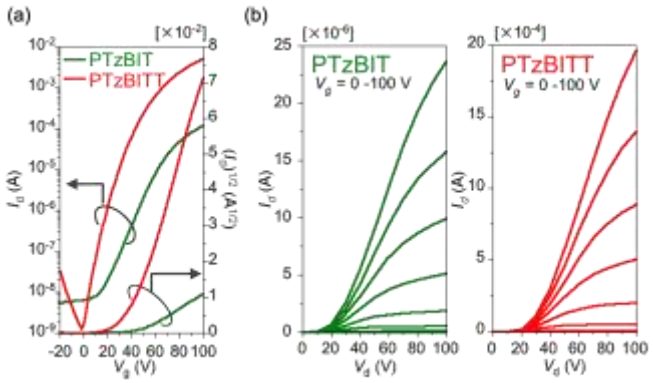


**Figure 5.** (a) Transfer curves of the OFET devices using PTzBIT (green line) and PTzBITT (red line). (b) Output curves of the OFET devices: PTzBIT and PTzBITT. The devices were annealed at 200 °C for 30 min.

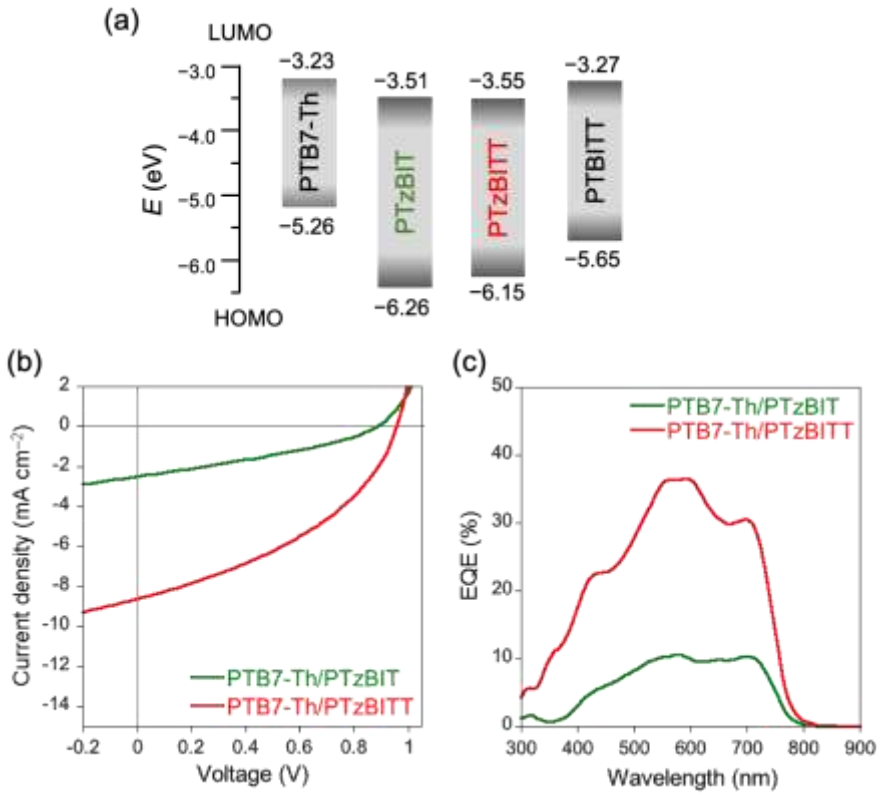


**Figure 6.** (a) Energy diagrams of PTB7-Th, PTzBIT, PTzBITT, and PTBITT. (b,c) Photovoltaic characteristics of the cells based on TzBI polymers as the n-type material: (b) *J*–*V* curves, (c) EQE spectra.

**Table 2.** OFET[a] and OPV properties.[b]

| polymer | $\mu_e$ (cm$^2$ V$^{-1}$ s$^{-1}$)[c] | $I_{on}/I_{off}$[d] | $J_{SC}$ (mA cm$^{-2}$) | $V_{OC}$ (V) | FF | PCE (%)[e] |
|---|---|---|---|---|---|---|
| PTzBIT | $1.1 \times 10^{-3}$ | $10^6$ | 2.49 | 0.88 | 0.33 | 0.71 |
| PTzBITT | 0.038 | $10^7$ | 8.61 | 0.96 | 0.40 | 3.30 |

[a]Bottom-gate bottom-contact device was used. [b]PTB7-Th was used as the p-type material. [c]Maximum electron mobility. [d]Current on/off ratio. [e]Maximum power conversion efficiency.

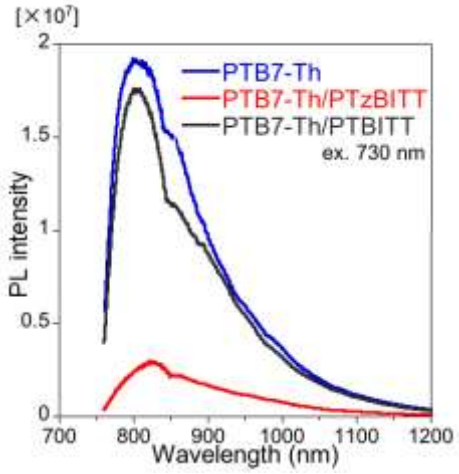


**Figure 7.** PL spectra of the PTB7-Th neat film, and PTB7-Th/PTzBITT and PTB7-Th/PTBITT blend films excited at 730 nm.

## CONCLUSIONS

We have designed and synthesized a new electron-deficient unit, TzBI, and TzBI-based copolymers. The polymers had relatively deep LUMO energy levels of below −3.5 eV, along with relatively wide optical bandgaps of around 1.9 eV. Thus, the polymers nicely match p-type semiconducting polymers with narrow optical bandgaps. We found that the main chains of the polymers were strongly packed with *d*-spacings of ca. 3.5 Å, leading to good crystallinity. The TzBI-based polymers functioned as n-type materials, as they provided electron mobilities of as high as 0.04 $cm^2\ V^{-1}\ s^{-1}$ in OFET devices. All-polymer OPVs that used TzBI-based polymers as the n-type material blended with PTB7-Th that has an optical bandgap of 1.58 eV as the p-type material also showed clear photovoltaic performance with reasonably high PCEs of up to 3.3%. These results indicate that TzBI is a promising building unit for n-type semiconducting polymers. Further studies on the optimization of the molecular structure, synthetic procedure to have higher molecular weights, and device performances are currently underway.

ASSOCIATED CONTENT

**Supporting Information**.

The Supporting Information is available free of charge on the ACS Publications website at DOI: xxx.

Materials, synthetic details, NMR spectra of the compounds, instrumentation, device fabrication, DSC thermograms, UV-vis absorption spectra, 2D-GIXD data, OFET data, OPV data, and AFM images.

AUTHOR INFORMATION

**Corresponding Author**

*E-mail: iosaka@hiroshima-u.ac.jp

**Author Contributions**

[§] These two authors contributed equally to this work.

**ORCID**

Itaru Osaka: 0000-0002-9879-2098

ACKNOWLEDGMENT

This work was supported by the Advanced Low Carbon Technology Research and Development Program (ALCA) from JST (grant no. JPMJAL 1404) and KAKENHI from JSPS (16H04196). 2D GIXD experiments were performed at the BL46XU of SPring-8 with the approval of the Japan Synchrotron Radiation Research Institute (JASRI) (Proposal No. 2018A1747). The authors thank Dr. T. Koganezawa (JASRI) for the support on 2D GIXD measurements. The authors are grateful

to Professor Y. Ie (Osaka University) for his support and valuable discussion on OFET fabrication and measurements.

REFERENCES


1) Burroughes, J. H.; Bradley, D. D. C.; Brown, A. R.; Marks, R. N.; Mackay, K.; Friend, R. H.; Burns, P. L.; Holmes, A. B. Light-emitting Diodes based on Conjugated Polymers. *Nature* **1990**, *347*, 539–541.

2) Perepichka, I. F.; Perepichka, D. F.; Meng, H.; Wudl, F. Light-emitting Polythiophenes. *Adv. Mater*. **2005**, *17*, 2281–2305.

3) Horowitz, G. Organic Field-effect Transistors. *Adv. Mater*. **1998**, *10*, 365–377.

4) Klauk, H. Organic Thin-film Transistors. *Chem. Soc. Rev.* **2010**, *39*, 2643–2666.

5) Yu, G.; Gao, J.; Hummelen, J. C.; Wudl, F.; Heeger, A. J. Polymer Photovoltaic Cells: Enhanced Efficiencies via a Network of Internal Donor-acceptor Heterojunctions. *Science* **1995**, *270*, 1789–1791.

6) Fu, H.; Li, C.; Bi, P.; Hao, X.; Liu, F.; Li, Y.; Wang, Z.; Sun, Y. Efficient Ternary Organic Solar Cells Enabled by the Integration of Nonfullerene and Fullerene Acceptors with a Broad Composition Tolerance. *Adv. Funct. Mater*. **2019**, *29*, 1807006.

7) Yan, H.; Chen, Z.; Zheng, Y.; Newman, C.; Quinn, J. R.; Dötz, F.; Kastler, M.; Facchetti, A. A High-mobility Electron-transporting Polymer for Printed Transistors. *Nature* **2009**, *457*, 679–686.

8) Günes, S.; Neugebauer, H.; Sariciftci, N. S. Conjugated Polymer-based Organic Solar Cells. *Chem. Rev.* **2007**, *107*, 1324–1338.

9) Kim, T.; Kim, J. H.; Kang, T. E.; Lee, C.; Kang, H.; Shin, M.; Wang, C.; Ma, B.; Jeong, U.; Kim, T. S.; Kim, B. J. Flexible, Highly Efficient All-polymer Solar Cells. *Nat. Commun.* **2015**, *6*, 8547.

10) Quinn, J. T. E.; Zhu, J.; Li, X.; Wang, J.; Li, Y. Recent Progress in the Development of n-type Organic Semiconductors for Organic Field Effect Transistors. *J. Mater. Chem. C* **2017**, *5*, 8654–8681.

11) Lee, J. K.; Gwinner, M. C.; Berger, R.; Newby, C.; Zentel, R.; Friend, R. H.; Sirringhaus, H.; Ober, C. K. High-Performance Electron-Transporting Polymers Derived from a Heteroaryl Bis(trifluoroborate). *J. Am. Chem. Soc.* **2011**, *133*, 9949–9951.

12) Baeg, K. J.; Caironi, M.; Noh, Y. Y. Toward Printed Integrated Circuits based on Unipolar or Ambipolar Polymer Semiconductors. *Adv. Mater.* **2013**, *25*, 4210–4244.

13) Takimiya, K.; Osaka, I.; Nakano, M. $\pi$ -Building Blocks for Organic Electronics: Revaluation of "Inductive" and "Resonance" Effects of $\pi$-Electron Deficient Units. *Chem. Mater*. **2014**, *26*, 587–593.

14) Zhang, M.; Guo, X.; Ma, W.; Ade, H.; Hou, J. A Polythiophene Derivative with Superior Properties for Practical Application in Polymer Solar Cells. *Adv. Mater.* **2014**, *26*, 5880−5885.

15) Osaka, I.; Takimiya, K. Naphthobischalcogenadiazole Conjugated Polymers: Emerging Materials for Organic Electronics. *Adv. Mater.* **2017**, *29*, 1605218.

16) Kang, H.; Uddin, M. A.; Lee, C.; Kim, K. H.; Nguyen, T. L.; Lee, W.; Li, Y.; Wang, C.; Woo, H. Y.; Kim, B. J. Determining the Role of Polymer Molecular Weight for High-

Performance All-Polymer Solar Cells: Its Effect on Polymer Aggregation and Phase Separation. *J. Am. Chem. Soc.* **2015**, *137*, 2359–2365.

17) Zhan, X.;Tan, Z.; Domercq, B.; An, Z.; Zhang, X.; Barlow, S.; Li, Y.; Zhu, D.; Kippelen, B.; Marder, S. R. A High-Mobility Electron-Transport Polymer with Broad Absorption and Its Use in Field-Effect Transistors and All-Polymer Solar Cells. *J. Am. Chem. Soc.* **2007**, *129*, 7246–7247.

18) Zhou, E.; Nakano, M.; Izawa, S.; Cong, J.; Osaka, I.; Takimiya, K.; Tajima. K.; All-Polymer Solar-Cell with High Near-Infrared Response Based on a Naphthoditiophene Diimide (NDTI) Copolymer. *ACS Macro Lett.* **2014**, *3*, 872–875.

19) Saito, M.; Osaka, I.; Suda, Y.; Yoshida, H.; Takimiya, K. Dithienylthienothiophenebisimide, a Versatile Electron-Deficient Unit for Semiconducting Polymers. *Adv. Mater.* **2016**, *28*, 6921–6925.

20) Stalder, R.; Mei, J.; Subbiah, J.; Grand, C.; Estrada, L. A.; So, F.; Reynolds, J. R. n-Type Conjugated Polyisoindigos. *Macromolecules* **2011**, *44*, 6303–6310.

21) Dou, C.; Long, X.; Ding, Z.; Xie, Z.; Liu, J.; Wang, L. An Electron-Deficient Building Block Based on the B←N Unit: An Electron-Acceptor for All-Polymer Solar Cells. *Angew. Chem. Int. Ed.* **2016**, *55*, 1436–1440.

22) Fei, Z.; Han, Y.; Martin, J.; Scholes, F. H.; Al-Hashimi, M.; AlQaradawi, S. Y.; Stingelin, N.; Anthopoulos, T. D.; Heeney, M. Conjugated Copolymers of Vinylene Flanked Naphthalene Diimide. *Macromolecules* **2016**, *49*, 6384–6393.

23) Zhao, Z.; Yin, Z.; Chen, H.; Zheng, L.; Zhu, C.; Zhang, L.; Tan, S.; Wang, H.; Guo, Y.; Tang, Q.; Liu, Y. High-Performance, Air-Stable Field-Effect Transistors Based on Heteroatom-Substituted Naphthalenediimide-Benzothiadiazole Copolymers Exhibiting Ultrahigh Electron Mobility up to 8.5 cm $V^{-1}$ $s^{-1}$. *Adv. Mater.* **2017**, *29*, 1602410.

24) Chen, Z.; Zheng, Y.; Yan, H.; Facchetti, A. Naphthalenedicarboximide- vs Perylenedicarboximide-Based Copolymers. Synthesis and Semiconducting Properties in Bottom-Gate N-Channel Organic Transistors. *J. Am. Chem. Soc.* **2009**, *131*, 8–9.

25) Guo, X.; Zhou, N.; Lou, S. J.; Hennek, J. W.; Ortiz, R. P.; Butler, M. R.; Boudreault, P. L. T.; Strzalka, J.; Morin, P. O.; Leclerc, M.; Navarrete, J. T. L.; Ratner, M. A.; Chen, L. X.; Chang, R. P. H.; Facchetti, A.; Marks, T. J. Bithiopheneimide-Dithienosilole/Dithienogermole Copolymers for Efficient Solar Cells: Information from Structure−Property−Device Performance Correlations and Comparison to Thieno[3,4-c]pyrrole-4,6-dione Analogues. *J. Am. Chem. Soc.* **2012**, *134*, 18427–18439.

26) Guo, X.; Ortiz, R. P.; Zheng, Y.; Hu, Y.; Noh, Y. Y.; Baeg, K. J.; Facchetti, A.; Marks, T. J. Bithiophene-Imide-Based Polymeric Semiconductors for Field-Effect Transistors: Synthesis, Structure-Property Correlations, Charge Carrier Polarity, and Device Stability. *J. Am. Chem. Soc.* **2011**, *133*, 1405–1418.

27) Shi, Y.; Guo, H.; Qin, M.; Zhao, J.; Wang, Yuxi.; Wang, H.; Wang, Yulun; Facchetti, A.; Lu, X.; Guo, X. Thiazole Imide-Based All-Acceptor Homopolymer: Achieving High-Performance Unipolar Electron Transport in Organic Thin-Film Transistors. *Adv. Mater.* **2018**, *30*, 1705745.

28) Shi, Y.; Guo, H.; Qin, M.; Wang, Yuxi.; Zhao, J.; Sun, H.; Wang, H.; Wang, Yulun; Zhou, X.; Facchetti, A.; Lu, X.; Zhou, M.; Guo, X. Imide-Functionalized Thiazole-Based Polymer Semiconductors: Synthesis, Structure−Property Correlations, Charge Carrier Polarity, and Thin-Film Transistor Performance. *Chem. Mater*. **2018**, *30*, 7988–8001.

29) Sun, H.; Tang, Y.; Guo H.; Uddin, M. A.; Ling, S.; Wang R.; Wang, Y.; Zhou, X.; Woo, H. Y.; Guo, X.; Fluorine Substituted Bithiophene Imide-Based n-Type Polymer Semiconductor for High-Performance Organic Thin-Film Transistors and All-Polymer Solar Cells. *Solar RRL*, **2019**, *3*, 1800265.

30) Sun, H.; Tang, Y.; Koh, C. W.; Ling, S.; Wang, R.; Yang, K.; Yu, J.; Shi, Y.; Wang, Y.; Woo, H. Y.; Guo, X. High-Performance All-Polymer Solar Cells Enabled by an n-Type Polymer Based on a Fluorinated Imide-Functionalized Arene. *Adv. Mater*. **2019**, *31*, 1807220.

31) Wang, Y.; Yan, Z.; Guo, H.; Uddin, M. A.; Ling, S.; Zhou, X.; Su, H.; Dai, J.; Woo, H. Y. Guo, X. Effects of Bithiophene Imide Fusion on the Device Performance of Organic Thin-Film Transistors and All-Polymer Solar Cells. *Angew. Chem. Int. Ed*. **2017**, *56*, 15304–15308.

32) Osaka, I; Kakara, T; Takemura, N; Koganezawa, T; Takimiya, K. Naphthodithiophene-Naphthobisthiadiazole Copolymers for Solar Cells: Alkylation Drives the Polymer Backbone Flat and Promotes Efficiency. *J. Am. Chem. Soc.* **2013**, *135*, 8834–8837.

33) Rogers, J. T.; Schmidt, K.; Toney, M. F.; Kramer, E. J.; Bazan, G. C. Structural Order in Bulk Heterojunction Films Prepared with Solvent Additives. *Adv. Mater*. **2011**, *23*, 2284–2288.

TOC figure